



## **LASERLAB-EUROPE**

### **The Integrated Initiative of European Laser Research Infrastructures III**

**Grant Agreement number: 284464**

**WP33**

**European Research Objectives on Lasers for Industry, Technology and Energy (EURO-LITE)**

**Deliverable number D33.7**

#### **Report on contrast enhancement by tailoring of pump/signal pulse temporal/energy characteristics**

**Lead Beneficiary:**

**VILNIAUS UNIVERSITETAS - VULRC**

**Due date: 31/05/2014**

**Date of delivery: 12/05/2014**

**Project webpage: [www.laserlab-europe.eu](http://www.laserlab-europe.eu)**

<i>Deliverable Nature</i>	
R = Report, P = Prototype, D = Demonstrator, O = Other	R
<i>Dissemination Level</i>	
PU = Public PP = Restricted to other programme participants (incl. the Commission Services) RE = Restricted to a group specified by the consortium (incl. the Commission Services) CO = Confidential, only for members of the consortium (incl. the Commission Services)	PP

## Abstract / Executive Summary

We report on the method of picosecond pulse envelope shaping based on pulse temporal profile transformations during the cascade second harmonic (SH) generation. It was demonstrated theoretically and experimentally that under a particular SH generation condition, Gaussian pulses can be converted to pulses of fundamental and second harmonics with the super-Gaussian temporal profile. The use of flat top pulses as a pump for high gain OPCPA system stages minimizes the effect of seed spectrum narrowing and allows reducing the energy of an amplified parametric fluorescence which deteriorates the final pulse contrast. This flat top pulse formation technique have been employed in TW-class OPCPA system driven by tandem femtosecond Yb:KGW and picosecond Nd:YAG lasers and producing high spatio-temporal quality output pulses with pulse duration of  $\sim 9$  fs and energy up to 35 mJ. The fraction of amplified parametric fluorescence background energy was measured to be smaller than  $3 \times 10^{-4}$ .

## B. Deliverable Report

### 1 Introduction

OPCPA systems based on non-collinear parametric amplification provides amplification bandwidths sufficient for formation of sub-10 fs pulses with ultrahigh peak powers, however both total gain, amplified pulse spectral bandwidth and contrast sensitively depend on temporal shape of the pump pulses. In most cases a pump pulse with a Gaussian temporal profile is used. If the seed and pump pulses are of comparable duration, the gain along the chirped seed pulse is non-uniform and usually leads to narrowing of amplified pulse spectrum. If a uniform gain across spectral signal bandwidth is to be achieved, the pump pulse has to be significantly longer than the seed pulse in order to keep the pump intensity approximately constant during amplification. In this case, however, a large fraction of the pump energy is discarded, thereby lowering the overall efficiency of the parametric amplification process. Additionally, the imperfect overlap will lead to the generation of fluorescence at those points in time, where there is no or only very little seed light available.

In the majority of works devoted to the development of sub-10 fs OPCPA systems, the main source of the broadband seed for the parametric amplification in vicinity of 800 nm was the output of a broadband mode-locked Ti:sapphire oscillator. In this case the OPCPA output pulse often exhibits a substantial uncompressible amplified parametric fluorescence (APF) background due to small seed energy. The scaling of the seed energy by employment of the Ti:sapphire amplifier in combination with the noble gas-filled hollow core fiber has led to a significant improvement in the output pulse contrast reducing APF caused background level down to  $10^{-10}$ . However, this technique does not eliminate temporal pedestal consisting of amplified spontaneous emission (ASE) coming from the Ti:sapphire frontend that is amplified within temporal window of OPCPA pump. Elimination of this background requires use of a cross-polarized wave generation (XPW) technique or a plasma mirror (PM) that introduces significant energy losses.

### 2 Objectives

Within the scope of EURO-LITE project VULRC is developing the high contrast OPCPA system for generation multi-mJ few cycle pulses at 1 kHz repetition rate. Study of nonlinear optics methods for ps pump pulse shaping in time and space domain, generation background-free seed pulses providing contrast, energy conversion enhancement in OPCPA systems is a main objective of this research. The purpose of this deliverable is to report on the results obtained exploring possibilities for flat-top temporal profile pump pulse formation using the cascade second harmonic generation processes and testing this technique in OPCPA system driven by tandem femtosecond Yb:KGW and picosecond Nd:YAG lasers

### 3 Work performed / results / description

#### Computer simulations of flat top picosecond pulse formation by cascade second harmonic generation

The pump pulses with a hipper Gaussian temporal profile and a duration comparable to that of the seed pulse can provide a uniform gain for all seed spectral components, thereby avoiding spectral gain narrowing, increasing pump-to-signal conversion efficiency and improving amplified pulse contrast ratio in respect to amplified parametric fluorescence (APF) background. There are number of techniques for shaping of ns or fs pulses based on application of fast optoelectronics, spatial light modulators, acousto-optic programmable dispersive filters. Flat top pulses of 30-100 ps can be obtained by pulse stacking. However, the resultant pulse shape obtained using this method is extremely sensitive to mechanical and thermal perturbations on the interferometric scale.

The main idea of our approach for the flat-top pulse formation could be presented as follows. In a second harmonic generation process the temporal profile of the fundamental harmonic (FH) pulse undergoes significant changes that are governed by the input pulse temporal profile and frequency conversion efficiency. In case of pulses with Gaussian temporal profile the growth of energy conversion to the second harmonic (SH) leads to flattening of residual fundamental pulse envelope and consequent formation of dip in the temporal pulse profile. The modified fundamental pulse leaving the first second harmonic generator could be used as a pump pulse in the second stage of harmonic generator. The SH generator pumped by flat top pulses will produce flat top pulses of second harmonic as well.

In order to find out the conditions for effective pulse envelope transformations employing cascade SH generators we have performed a numerical simulation of the three-wave parametric interaction using the symmetrized split-step method. According to the model the nonlinear crystal was divided into number of slices. Diffraction and material dispersion were accounted for in each slice independently from the nonlinearity of material. The linear propagation of the waves was handled in the Fourier space as

$$A_j(t, x, y, z + \Delta z) = \mathcal{F}^{-1} \left\{ S_j(w, k_x, k_y, z) \exp \left( -i \sqrt{k(w, k_x)^2 - k_x^2 - k_y^2} \Delta z \right) \right\} \quad (1)$$

where  $j=1$  and  $2$  indicate fundamental and second harmonic respectively;  $\mathcal{F}^{-1}$  denotes the inverse Fourier transformation and  $S_j(w, k_x, k_y, z)$  is the initial spectrum of the wave given by  $S_j(w, k_x, k_y, z) = \mathcal{F}\{A_j(t, x, y, z)\}$ . Dispersion and diffraction effects were accounted for via exponential term in Eq. (1), where  $k(w)$  describes the material dispersion. For the extraordinary wave the spatial walk-off was taken into account via  $k$  dependence on  $k_x$ , i.e. on propagation direction. The nonlinear step was performed using the fourth-order Runge-Kutta method for integration of the coupled wave equations (2) in the near field representation  $(t, x, y, z)$ ;

$$\frac{\partial A_1}{\partial z} = -i \frac{w_1^2}{k_1 c^2} d_{eff} A_2 A_1^* \quad (2)$$

$$\frac{\partial A_2}{\partial z} = -i \frac{w_2^2}{2k_2 c^2} d_{eff} A_1^2 \quad (3)$$

Numerical simulations were performed for the case of two stage cascaded SH generation employing a type-I (oo-e) phase matching DKDP crystals with a length  $L = 10$  mm in the first stage and  $L=20$  mm in the second stage of SH generator. The coefficients of Sellmeier equations were used and the effective second order nonlinear susceptibility was taken to be  $d_{eff} = 0.22$  pm/V. It was assumed that the FH pump pulse entering the SH generators have a Gaussian temporal profile with pulsewidth at FWHM of 70 ps.

Simulation results presented in Fig. 1a reveal that changes in temporal profile of the residual FH after the first stage of SH generation when increasing pump pulse intensity  $I_p$  are quite substantial. At pump intensity value of  $I_p = 4$  GW/cm<sup>2</sup> the FH pulse envelope takes flat top temporal profile exhibiting the pulse intensity plateau region of  $\approx 50$  ps (line (2) in

Fig.1a). Note, that in this case the pulse duration defined at FWHM increases up to 111 ps. Further increase of pump intensity results in progressively growing envelope modulation of the FH pulse (see lines (3), (4) in Fig.1a).

In the second step we have performed the computer simulation of the SH generation using the fundamental harmonic pulses depicted in Fig.1a as a pump for the second stage of the SH generator.

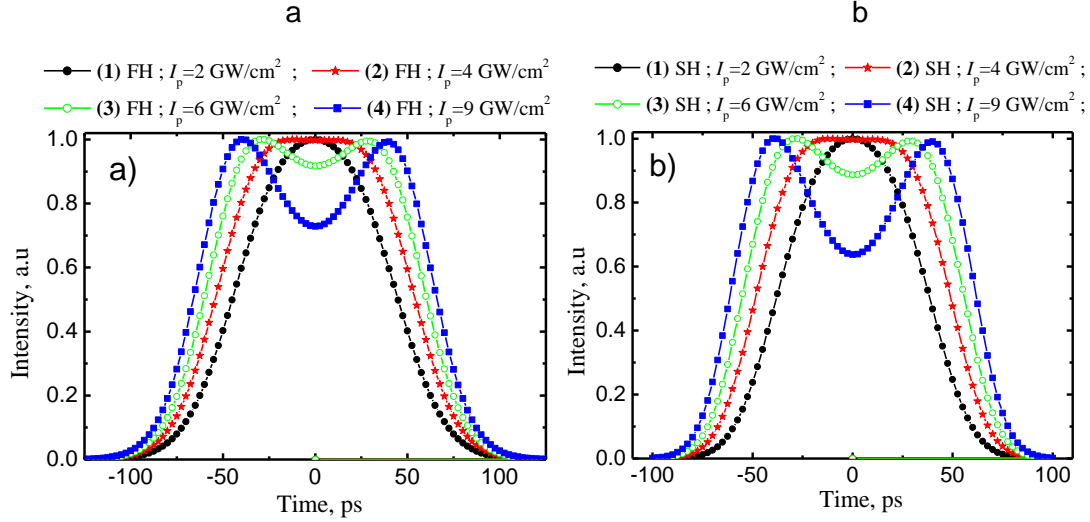


Fig. 1. (a) Temporal profiles of the residual FH after the first stage of the SH generator for different pump pulse peak intensities; (b) corresponding temporal profiles of the second harmonic after the second stage of the SH generator.  $I_p$  is the pump peak intensity at the first stage of the SH generator.

The simulation results, presented in Fig.1b., shows that the temporal profile of the SH pulse generated in the second stage tends to repeat the pump pulse temporal profile with modestly reduced pulse duration and increased temporal modulation. Also it is worth to mention that using the same approach and more than two SH generation stages the FH and the SH pulse flattening effect become more and more notable after each subsequent SH generation stage and the form of the pulse envelope approaches to the rectangular one.

Pulses exhibiting an intensity dip in their temporal profile could find an application as a pump for OPCPA systems also, providing an opportunity to achieve higher gain for the spectral component situated at the leading and the trailing edges of the seed pulse and obtain broader amplified pulse spectrum.

#### Experimental investigation of flat-top pulse formation

The experiment was carried out using Nd:YAG based amplification system developed for pumping of OPCPA. In our setup, schematically presented in Fig. 2, Yb:KGW fs oscillator (Light conversion, Ltd.) which provides pulses of a 60 fs duration and 9 nJ of energy at a 78 Mhz repetition rate was used as a seed source both for femtosecond Yb:KGW regenerative amplifiers and for picosecond Nd:YAG amplification system.

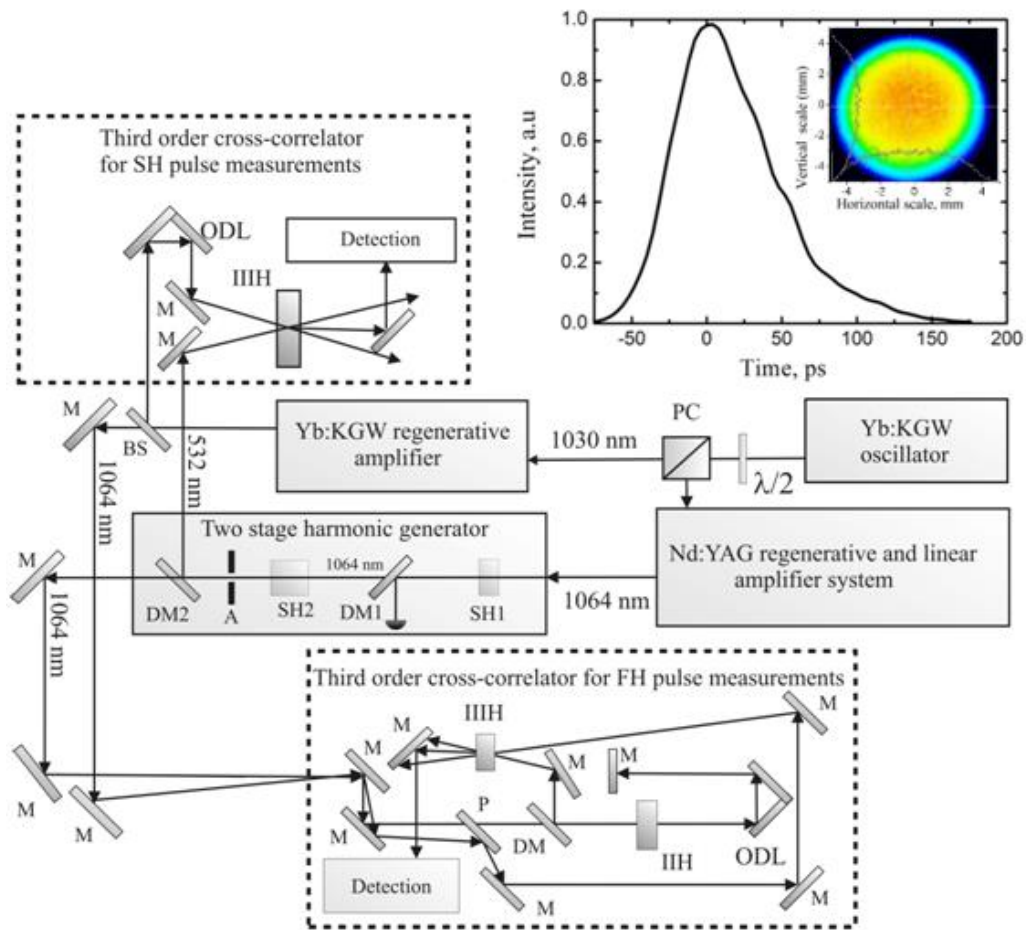


**Fig.2** Picosecond pulse shaping and measurement system: M – mirrors, ODL-optical delay line, SH1 – DKDP crystal (10 or 13 mm of length), SH2 – DKDP crystal 20 mm of length, SH and TH – the second and the third harmonic crystals for the pulse cross-correlation

Nd:YAG power amplifier boosted pulses energy up to 500 mJ at repetition rate of 10 Hz. The spatial shape of the output beam had a smooth intensity distribution (see inset in Fig.2) which was well approximated by the third order hyper-Gaussian function. In experiment the DKDP crystals of 10 mm or 13 mm length were used in the first stage of SH generator, while the length of the crystal in the second stage was 20 mm. All the crystals were cut for type I phase matching at polar angle  $\theta=36.6^\circ$  and azimuthal angle  $\varphi=45^\circ$ . The measurements of the temporal shape of the FH pulses were performed by using the third-order cross-correlator (Sequoia, Amplitude Technologies) designed for 1000–1150 nm wavelength range. We have modified the arrangement of the cross-correlator for the measurements of picosecond pulse temporal profile by setting up an additional beam path for  $\sim 300$  fs probe pulses delivered by PHAROS system

The experiment confirmed expectations that due to intensity dependent three wave parametric interaction the flattening of initial bell shaped FH pulse takes place and at certain pump intensity level the pulse envelope of residual FH becomes the flat-top shaped. Further increase of pump intensity and corresponding conversion efficiency to the SH leads to appearance of a dip in the pulse temporal envelope. The measured pulse temporal profiles were in good agreement with the results of computer simulations performed using actual pump pulse characteristics.

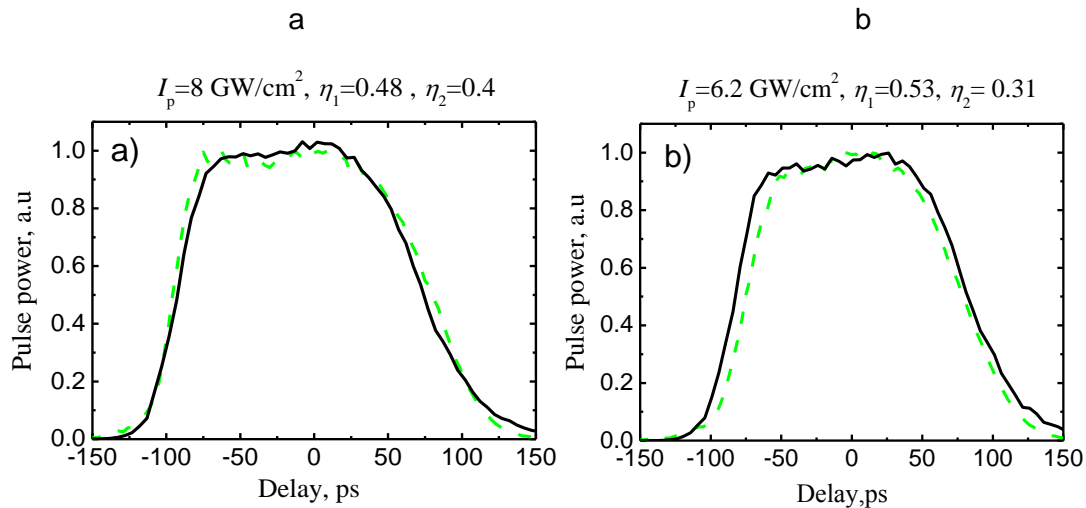


**Fig. 3** Flat top pulses from cascade SH generator using 10 mm (a) and 13 mm (b) long crystals in the first SH generation stage: solid lines – temporal profile of FH pulses, dashed lines – temporal profile of SH pulses.  $\eta_1$  and  $\eta_2$  indicate the conversion efficiency in the first and second stage of SH generator, respectively.

In Fig.3 the results of flattened pulse shape measurements performed acquiring the signal from whole the beam are presented. We have shown that at the particular the second harmonic generation conditions the 1064 nm pump pulses with temporal profile close to Gaussian and pulse width of ~75 ps at FWHM can be converted to pulses of the fundamental and the second harmonic with super-Gaussian temporal profile having intensity plateau region extending over ~ 100 ps time interval.

The main condition for flat top pulse formation is that the energy conversion efficiency in the first stage of harmonics generator should be around 45 – 50 %. The obtained results were roughly the same for both the DKDP crystal length of 10 mm and 13 mm. The only difference was that maximum pulse temporal profile flattening for the crystal of 13 mm was recorded at ~25 % lower pump pulse energy. So, the flat top pulse can be generated using nonlinear crystal of different length and attaining 45 – 50 % pump to the SH conversion efficiency by adjusting pump pulse intensity.

Flat top the second harmonic pulses at 532 nm were obtained in the second stage of SH generator (see Fig.11). The energy conversion efficiency to the SH in 20 mm long of DKDP crystal was in the range of 20 – 40% depending on pump pulse energy. The temporal structure of the ps second harmonic pulses, generated in the second SHG stage, was characterized by the home-made third-order cross-correlator in which 1030 nm femtosecond pulses from PHAROS system were used for the 532 nm picosecond pulses probing (see Fig. 2). The SH pulse temporal profiles measured for the different FH pulse intensities  $I_p$  at the entrance of two stage SH generator are presented in Fig. 13. Similar to results of computer simulations, in the case of flat-top pump pulses both the SH pulse duration and the width of the intensity plateau corresponds to those of the pump pulse with accuracy of < 95 %.



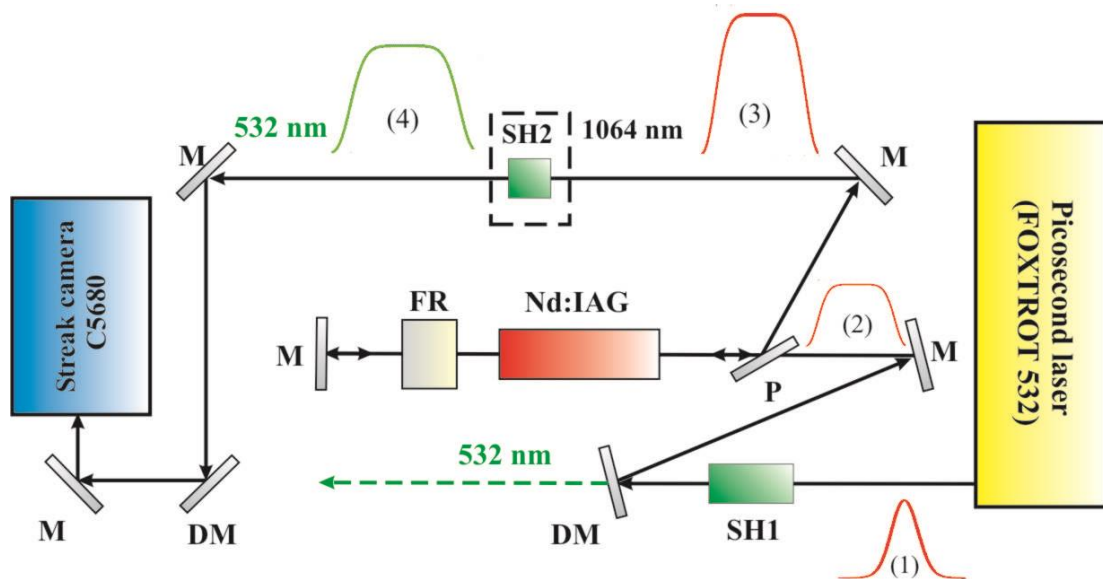


**Fig. 4** Picosecond pulse shaping – amplification system: SH1 and SH2 – second harmonic crystals, FR – Faraday rotator, M – mirrors, DM – Dichromatic mirrors, P – polarizer.

We also have examined the possibility for distortion-free amplification of flat top pulses in additional laser amplifier compensating in this way the  $\sim 50\%$  pulse energy losses taking place during second harmonic generation. The schematic of experimental set-up is presented in Fig.4. In case of pulses with Gaussian temporal profile (1) the growth of energy conversion to second harmonic (SH) leads to flattening of residual fundamental pulse envelope (2) and even to formation of dip in the temporal pulse profile. The modified fundamental pulse leaving the first second harmonic generator could be amplified and used as a pump pulse in the second stage of harmonic generators (SH2). The SH generator pumped by amplified flat top pulses (3) will produce flat top pulses of second harmonic as well (4). The main goal of the experiment was to clarify to which extent the amplification saturation effect distorts the temporal profile of amplified pulses.

The experimental results are presented in Fig.5. The experiment was carried out by pumping 10 mm of length LBO crystal (SH1) with 56 ps width (at FWHM) and 0.4 mJ of energy Gaussian pulses (line (1) in Fig. 15). Pulses having an intensity plateau region extending 50 ps time interval were formed (line (2)) when conversion efficiency in the SH1 was around 50 %. Shaped pulses were amplified in the double pass power amplifier up to 1.7 mJ of energy what corresponds to pulse intensity of  $I=1.28 \text{ GW/cm}^2$  and energy fluence of  $F=0.128 \text{ J/cm}^2$ . Then pulses were frequency doubled in the 3 mm length KTP crystal (SH2), Pulse profiles were measured with streak camera C5680 (Hamamatsu Photonics).

The results of the measurements presented in Fig.5 indicate that in our experimental conditions the changes in temporal profile during amplification are less than 2% ( see lines 2 and 3).

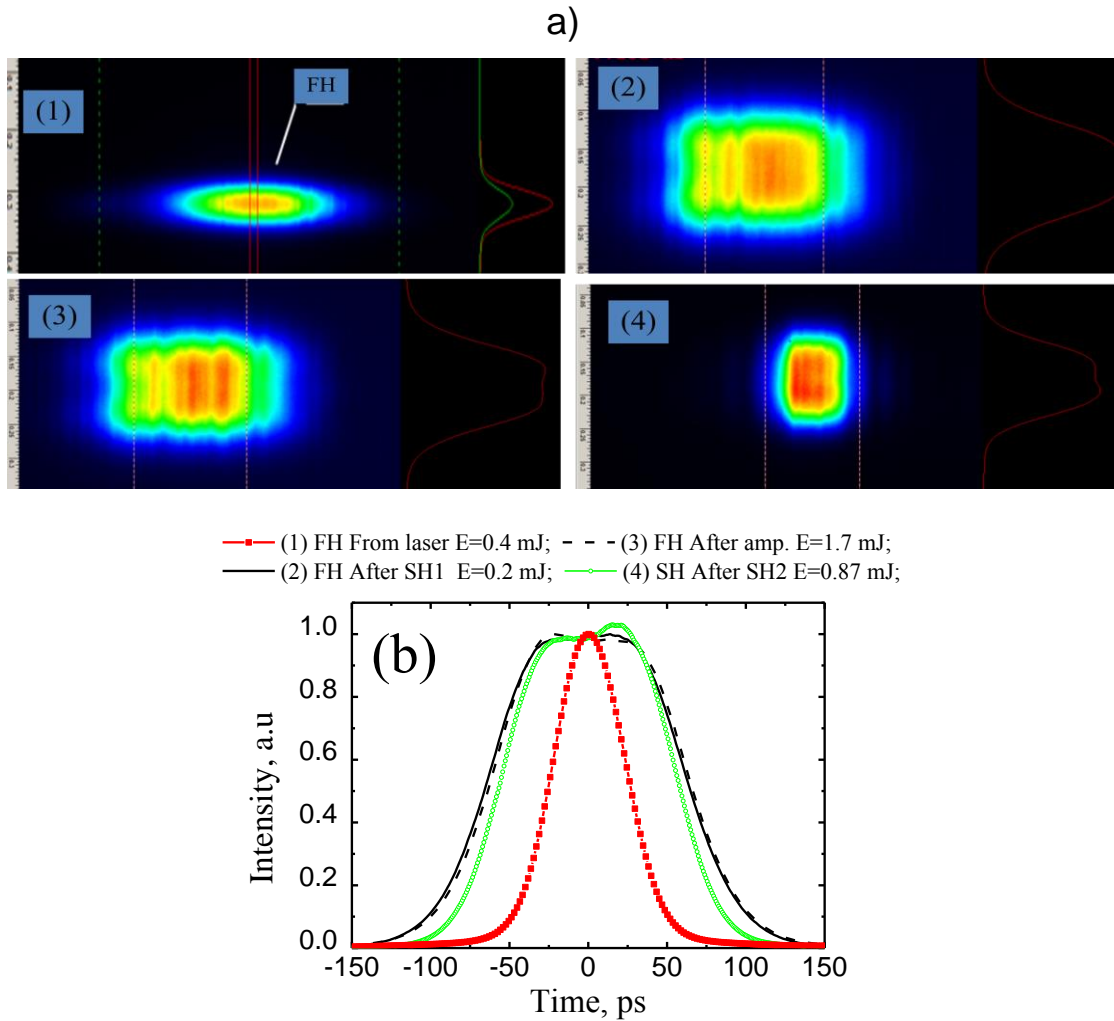


**Fig. 5** Picosecond pulse temporal profiles after subsequent pulse shaping-amplification stages.: a) Streak camera view ; b) Data extracted from streak camera view.

#### TW class OPCPA system pumped by fs/ps pulses

The flat-top pump pulse formation technique has been tested in OPCPA system pumped by tandem Yb:KGW and Nd:YAG lasers. The setup of our OPCPA system is outlined schematically in Fig. 6. The system can be conceptually divided into a non-collinear optical parametric pre-amplifier of white light continuum, pumped by femtosecond pulses (fs NOPA), and a high energy picosecond parametric amplifier.

A source of broadband and ASE-free seed pulses around 800 nm is a white light continuum (WLC) generated in a bulk materials by femtosecond pulses ytterbium-doped laser system, which automatically provides the possibility to perform seed generation and amplification in a femtosecond non-collinear optical parametric amplifier (NOPA). Employment of femtosecond pump pulses in the initial OPCPA stages is advantageous, since thinner crystals and narrower pump beams can be used, implying an increased amplification bandwidth and a reduced level of APF which is proportional to the pump beam area. It is also important to point out that the recompressed APF resides within the time window defined by the duration of the femtosecond pump pulse, since the contribution of APF arising in the subsequent picosecond amplifications stages is practically negligible.



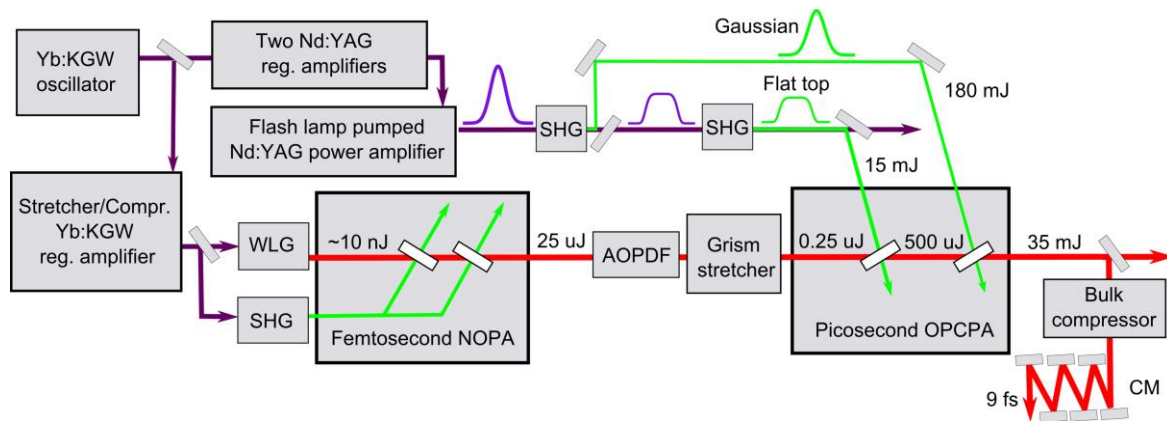


Fig. 6. Layout of the OPCPA system. WLG, white light continuum generation; SHG, second harmonic generation; AOPDF, acousto-optic programmable dispersive filter; CM, chirped mirrors.

The front end is based on a solid-state Kerr lens mode-locked Yb:KGW oscillator, which delivers 7 nJ, 80 fs pulses at 1030 nm. Most of the oscillator output is sent through a transmission grating stretcher and then used to seed an Yb:KGW regenerative amplifier (Light Conversion Ltd.), delivering up to 1 mJ pulses at 1 kHz. Also, using a polarizing spectrum splitter, a fraction of the oscillator pulse energy (12 pJ within 0.6 nm bandwidth at 1064 nm) is delivered to a Nd:YAG regenerative amplifier. Thus, by seeding the two amplifiers from one master oscillator, we realize an all-optical synchronization of the seed and pump pulses. The compressor of the Yb:KGW regenerative amplifier is detuned slightly to deliver down-chirped pulses of ~450 fs at full width half-maximum (FWHM). A few percent of the amplifier output are compressed in a 4 cm ZnSe rod and focused into a 4 mm sapphire plate to generate a smooth white light continuum. The main portion of the amplifier pulse was frequency doubled in a 0.7 mm thick BBO crystal and then used to pump the two stages of the fs NOPA. Using chirped pump pulses in the fs NOPA allows us to match the durations of the seed and the pump without any dispersion management of the white light continuum, thus minimizing the losses and making the system simpler and more compact. Parametric amplification is carried out in Type-I BBO crystals at a non-collinearity angle  $\alpha = 2.5^\circ$  and phase matching angle  $\Theta = 24.6^\circ$ . In order to minimize the parametric superfluorescence, the first femtosecond NOPA stage is operated in a low-gain regime, keeping the pump intensity ~3 times below the saturation level. The continuum pulses are amplified from ~10 nJ to 0.6 mJ by using 15 mJ pump pulses. The seed and pump beams were both focused to a spot size FWHM of ~140  $\mu\text{m}$  onto 2.5 mm BBO crystal. The second stage (1.8 mm BBO long, beam diameter 1 mm) are pumped by pulses of 300 mJ and increases the signal energy up to 25 mJ, while the spectrum (see Fig. 2(a)) corresponds to a Fourier-limited pulse duration of 6.7 fs.

The amplified seed pulses are sent to a compact grism based stretcher and then to the picosecond amplification stages. Pump pulses for ps parametric amplifiers was produced by Nd:YAG amplification system (EKSPLA Ltd.) comprising of regenerative and linear amplification stages. A two-stage cascaded second harmonic (SH) generation scheme was used for conversion of 380 mJ of the fundamental Nd:YAG harmonic (FH) pulse into two SH pulses with different temporal shapes. After the first SHG crystal (DKDP type I, 10 mm long), SH pulses with a nearly Gaussian envelope (70 ps FWHM) were generated with 50% efficiency. In the second SHG stage (DKDP type I, 20 mm long) the remainder of the FH pulse was used for generation of a flat-top SH pulse. The shapes of picosecond pump pulses measured by the cross-correlation technique using femtosecond pulses from the Yb:KGW laser as a probe are presented in Fig. 7(b,c).

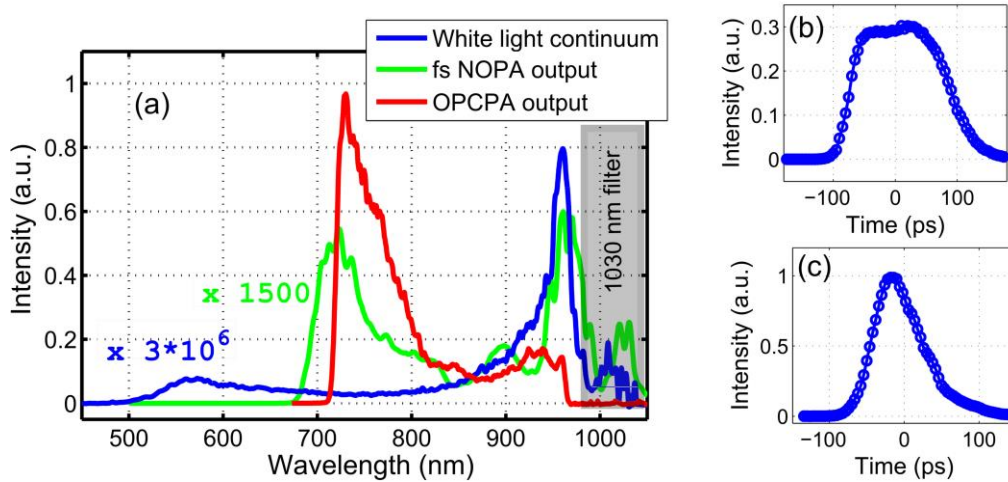


Fig. 7. (a) White light continuum (blue curve) and the spectra after amplification in fs NOPA (green curve) and in OPCPA (red curve).

Temporal profiles of the pump pulses used in the first (b) and the second (c) picosecond OPCPA stages. Both picosecond OPCPA stages are based on 5 mm long BBO crystals. The first stage, pumped with 15 mJ, 100 ps flat-top pulses focused to a spot of 0.8 mm diameter (FWHM), amplifies the seed pulses to 0.5 mJ. Next, the signal beam is expanded to a diameter of 8 mm (FWHM) to match main pump beam and amplified to 35 mJ in the second OPCPA stage. This stage is operated at low gain and strong saturation to avoid narrowing the signal spectrum. A typical OPCPA output spectrum is shown in Fig. 7(a) (red curve). Wavelengths above 970 nm have undesirable spectral phase modulation, caused by a filter inserted after the WLC generator to block the 1030 nm pump pulses. Therefore, these wavelengths are intentionally filtered out in the grisms. The asymmetry of the spectrum results from the slight asymmetry of the pump pulse in the last OPCPA stage and from the dispersion of the stretcher, since in our case, the shorter wavelengths are more dispersed in time as compared to longer ones, and thus interact with more pump energy per unit spectral interval.

In our system, we employ the down-chirped pulse amplification technique. The stretching module consists of an acousto-optic programmable dispersive filter (AOPDF) with a 45 mm-long TeO<sub>2</sub> crystal (Dazzler, Fastlite), followed by a home-built grism stretcher for flexible dispersion control. The stretcher is composed of SF-10 prisms with an apex angle of 19 degrees and reflective gratings with a groove density of 300 grooves/mm. At the exit of the stretcher, the seed pulses have a duration of ~50 ps. The achievable duration of the stretched seed pulses was limited by the aperture of our grisms. However, it would be desirable to stretch the seed pulses more in order to match the ~100 ps flat-top pump pulses better. The compressor consists of several rods of H-ZF52A glass (SF-57 equivalent), adding up to a total length of 420 mm, and a 100 mm of fused silica (FS). The final stage of the compression is performed by 6 bounces from the chirped mirrors (Optida Ltd.) with a group delay dispersion (GDD) of approximately +50 fs<sup>2</sup>/bounce. Due to the small aperture of the H-ZF57A glass rods available in our laboratory, the OPCPA output was attenuated to 50 mJ before being sent to the compressor, thus avoiding nonlinear propagation effects.

The compressed pulses were characterized simultaneously by chirpscan, utilizing the AOPDF in the stretcher, and Frequency Resolved Optical Gating (FROG). The apparatus we have used allowed us to perform SHG FROG and chirpscan measurements in the same optical setup, thus it is meaningful to compare the results obtained by these two methods. The chirpscan trace of the compressed pulse is shown in Fig. 8(a). The trace exhibits good left-to-right symmetry, which is a strong indication of a nearly transform-limited pulse, thus even using the stationary phase approximation one should get a reasonable estimate of the spectral phase, shown in Fig. 8(b) (curve no. 3). Applying this phase to the measured OPCPA output spectrum yields a pulse that is virtually indistinguishable from the transform-limited one. The FROG trace was measured without altering dispersion settings of the

system and the corresponding FROG inversion results are shown in Fig. 4(b)-4(d). The FROG retrieval error was 1.8% on a 128x128 grid. Although the FROG measurement shows a certain amount of residual chirp, the measured pulse duration still differs by less than 9% from the transform limit and ~60% of the pulse energy is delivered within a  $\pm 5$  fs temporal window.

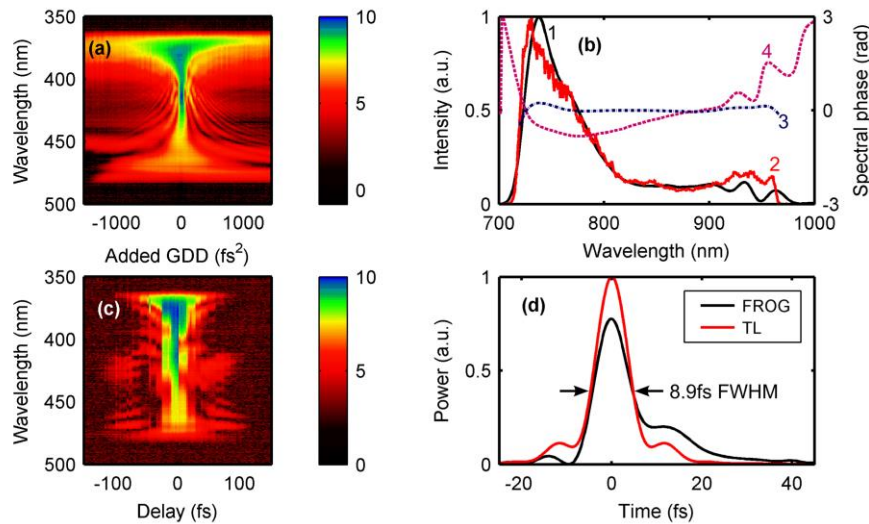


Fig. 8. Characterization of the compressed pulse: (a) Chirpscan trace. (b) Pulse spectra as retrieved by FROG (1) and measured independently (2). Spectral phases as retrieved from chirp scan (3) and FROG (4) measurements. (c) FROG trace. (d) Temporal pulse shape as measured by FROG and a transform-limited pulse (TL) with the same spectrum.

In order to inspect the level of amplified superfluorescence, we have measured the OPCPA output energy while the white light continuum was blocked. We found that this energy is mostly determined by the pump intensity in the first amplification stage of the fs NOPA and was lower than 10  $\mu$ J (<0.03% of the amplified signal energy) under normal operating conditions.

## 4 Conclusions

We have explored possibilities for flat-top picosecond pulse formation by using the cascade second harmonic generation processes. It was shown that at the particular second harmonic generation conditions the 1064 nm pulses with temporal profile close to Gaussian and pulsewidth of ~75 ps can be converted to pulses of the fundamental and the second harmonic with super-Gaussian temporal profile having intensity plateau region extending over ~ 100 ps time interval. The main condition for flat top pulse formation is that the energy conversion efficiency in the first stage of harmonics generator should be around 45-50%. Proposed shaping method is particularly suitable for the application in the multistage OPCPA pumping by the second harmonic of Nd:YAG lasers. Using this method the residual radiation of the fundamental harmonic after SH generation in the first stage is effectively used in the second SH generation stage for the formation of pump pulses with sufficiently broad intensity plateau region. This method of pump pulse formation was tested in 10 Hz repetition rate OPCPA system. The fraction of the output pulse background energy with reference to energy of main pulse was measured to be smaller than  $3 \times 10^{-4}$ . Experimental determination of OPCPA output contrast parameters at different temporal windows before the main pulse still have to be done after setting in operation 1 kHz repetition rate OPCPA system that is under development.

## 5 References/Publications

1. J. Adamonis, R. Antipenkov, J. Kolenda, A. Michailovas, A.P. Piskarskas, A. Varanavičius, A. Zaukevičius, "Formation of flat-top picosecond pump pulses for OPCPA systems by cascade second harmonic generation", *Lith. J. Phys.* **53**, 193–202 (2012) (Open access)
2. T. Stanislauskas, R. Budriūnas, R. Antipenkov, A. Zaukevičius, J. Adamonis, A. Michailovas, L. Giniūnas, R. Danielius, A. Piskarskas, A. Varanavičius, "Table top TW-class OPCPA system driven by tandem femtosecond Yb:KGW and picosecond Nd:YAG lasers", *OPTICS EXPRESS*, 22, 1865-1870 (2014)  
DOI:10.1364/OE.22.001865 (open access)